On Mathematical Folding of Curved Crease Origami: Sliding Developables and Parametrizations of Folds into Cylinders and Cones

Klara Mundilova

Institute for Discrete Mathematics and Geometry, TU Wien

Abstract

Motivated by the art of curved crease origami we study mathematical models for folding ideal paper along curved creases. We approach the problem of finding mathematical descriptions in terms of developable surfaces of those shapes which can be folded from real paper but where its rigorous description is often unknown. For that we investigate a particular one-parameter family of surfaces isometric to a given planar surface patch. For each such surface we parametrize the crease curves which fold those surfaces into cylinders and cones. We apply our methods to explore curved crease origami designs, such as tessellations of the plane and cylinders.

Keywords: developable surfaces, curved creases, origami, folding

1. Introduction

This paper is a generalization of methods utilized in Mundilova and Wills [1] for the geometric description of a by hand easily obtained shape appearing in the sculpture "Attraction" by Susan Latham. In this sculpture, two overlapping discs, the so called Vesica Piscis, are folded along their inner circle segments, so that the outer coincide, see Fig. 1.

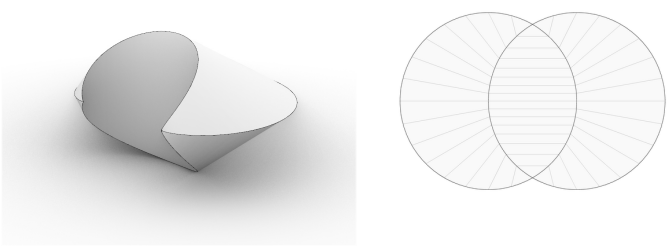

Figure 1: Folded Vesica Piscis used in Susan Lathams sculpture.

However, mathematical paper folding is more restrictive than folding real paper. Mathematically ideal paper is infinitely thin, not stretchable and allows just creases that exactly fit together in the development. Paper or other "non-stretchable" sheets of materials on the other hand seem to allow additional little creases or imperfections in stiffness. For example, the pleated hyperbolic paraboloid seems foldable, but Demaine et al. showed in [2] that this shape does not mathematically exist without additional creases. The existence of other objects, such as the pleated circular folding of an annulus, are still open problems, although strong numerical evidence for its existence was found by Dias et al. [3, 4]. By determining the folded Vesica Piscis parametrization, Mundilova and Wills [1] proved its existence.

In this paper, we give a generalization of the two steps utilized to parametrize the folded Vesica Piscis. Firstly, we investigate the generation of shapes isometric to a given development by keeping the surface boundaries planar. Then, we derive formulas for the crease curves that fold a given surface into a cylinder or a cone. The hereby obtained methods can be used for the explicit mathematical design of shapes with curved creases and we give some examples in Section 6.

2. Prior work

One of the most influential curved crease paper folding designers was David Huffman. Insights in his work are given by Demaine et al. [5] and Koschitz [6]. Huffman's investigatigations of the local mathematical behaviour of paper in [7] were succeeded by Fuchs and Tabachnikov [8] who established conditions for smoothly folded paper. Namely, the intrinsic curvatures of the crease curve w.r.t. the adjacent developable strips must coincide in order for them to fit together in the developed state. This can be also reformulated in terms of the osculating plane of the curve being the bisector of the tangent planes of the two adjacent surfaces in every point. Demaine et al. [9, 10] further studied the relationship between creases and rulings, in particular in connection with Huffman's designs. The latter gives a complete characterization of the existence of designs with constant fold angles between cylinders and cones.

Wunderlich [11, 12, 13, 14] gives a geometric description of pseudo geodesics, i.e., surface curves whose osculating planes enclose a constant angle with the surface tangent plane, on cylinders and cones. His work thus gives insight into creases of constant angle where at least one surface is a cylinder or a cone. Another approach is pursued by Röschel [15, 16], where a geometric characterization of creases between pairs of cylinders and pairs of cones is obtained. More applied studies on creases into cylinders were done in the context of shoulders in packaging machines by Boersma and Molenaar [17].

As curved creases have various applications, there have been different computational approaches. Solomon et al. [18] introduce an optimization setting to enforce exact developability of discretized surfaces. Ghassaei's online available tool "Origami Simulator", see [19], can compute discretized shapes with curved creases online. Rigid foldable stuctures with one degree of freedom based on discretized folds along space curves are discussed by Tachi [20, 21]. Moreover, Mitani's tools for a restricted, but

Email address: klara.mundilova@tuwien.ac.at (Klara Mundilova)

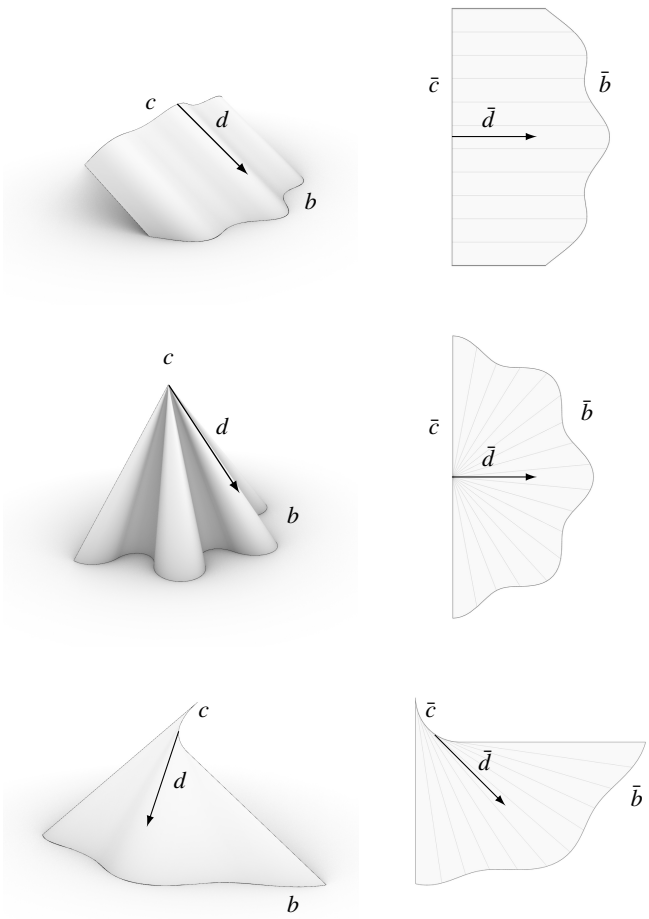

Figure 2: The basic types of developable surfaces: cylinder, cone and envelope of tangents of a space curves.

still intriguing, class of column-shaped origami designs obtained by discretized planar reflections are described in [22, 23] .

Smooth approaches were pursued by Kilian et al. [24] where they propose an algorithm that approximates a given target surface with developable patches connected along curved creases. A tool that is based on optimization of quadratic functions for the interactive design of developable surfaces with curved creases was introduced by Tang et al. [25]. In addition, Rabinovich et al. [26] present an algorithm for modelling developable surfaces and Kirigami with discrete geodesic nets. Another perspective on curved folds is given by Kilian [27], where an algorithm for the computation of string mechanisms that actuate a desired folding motion is presented.

We would also like to mention D-Forms, which are three dimensional shapes, that are obtained by gluing two planar patches of equal perimeter along their boundaries. They were introduced by Wills [28] and formalized by Pottmann and Wallner [29]. The existence of D-Forms obtained by planar patches with convex smooth boundaries was proven by Demaine et al. [30]. Recall, although their generation is manually feasible, the mathematical description of such shapes is very challenging. However, an example is given by Stachel [31].

3. Notation

It is well known that developable surfaces i.e., surfaces that are isometric to the plane, are composed by cylinders, cones and tangent surfaces.

As those are ruled surfaces with the property that the tangent plane is constant along each ruling, we will parametrize these surface patches with a (possibly degenerated) curve $c(s)$, a normalized direction vector $d(s)$ and a ruling length function $l(s)$ by

$$\Gamma(s,t) = c(s) + td(s) \quad \text{with} \quad s \in [s_0, s_1] \quad \text{and} \quad t \in [0, l(s)].$$

We can make the following assumptions: In case of a cylinder, $d = \text{const}$ and we assume c to be a profile curve, i.e., being contained in a plane orthogonal to d. In case of a cone, we denote the vertex of the cone by c and in case of a tangent developable, c denotes the curve of regression and $d = \frac{c'}{|c'|}$, where the prime denotes the derivative w.r.t. the parameter s. Furthermore, we refer to the second boundary of the surface patch which is not a ruling by $b(s) = c(s) + l(s)d(s)$.

Given such a developable surface, it is straightforward how to unroll it to the plane, see e.g., [29]. We will indicate the corresponding developments with bars, i.e.,

$$\bar{\Gamma}(s,t) = \bar{c}(s) + t\bar{d}(s) \quad \text{with} \quad s \in [s_0, s_1] \quad \text{and} \quad t \in [0, l(s)].$$

Furthermore, we denote the x, y and z-coordinates by a subscript, e.g., $c = (c_x, c_y, c_z)$.

4. Isometric Deformations of Developable Surfaces

In this section, we propose a construction of a developable surface which is isometric to a given planar surface patch. Given information about the intended ruling structure, we guide a deformation process by keeping one boundary curve planar.

4.1. Cylinders

Let $\bar{\Gamma}$ be a planar cylindrical patch (i.e., $\bar{d} = \text{const}$) where the profile curve $\bar{c}$ is parametrized by arc length. We determine the parametrization of a profile curve c of a cylinder Γ which is isometric to $\bar{\Gamma}$ by elevating its normalized ruling direction d while keeping its boundary b in the xy-plane:

Let us w.l.o.g. assume that the ruling direction is given by

$$d = (\cos\phi, 0, \sin\phi).$$

From the planarity of b we conclude

$$0 = b_z = c_z + ld_z \quad \Longrightarrow \quad c_z = -l\sin\phi.$$

As c is contained in a plane perpendicular to d,

$$k = d \cdot c = c_x\cos\phi + c_z\sin\phi,$$

is a constant which determines the distance of the plane from the origin. We therefore obtain

$$c_x = \frac{1}{\cos\phi}\left(k + l\sin^2\phi\right).$$

Finally, we ensure the isometry by $|c'| = |\bar{c}'| = 1$, i.e.,

$$c_y' = \sqrt{1 - c_x'^2 - c_z'^2} = \sqrt{1 - l'^2\tan^2\phi}.$$

The square root is real if

$$\tan^2\phi \le \frac{1}{l'^2} \quad \text{for all } s \in [s_0, s_1],$$

and therefore if

$$|\phi| \le \phi_{\max} = \arctan \min_{s\in[s_0,s_1]} \frac{1}{l'^2}.$$

For $\phi_{\max} > 0$, the elevation angle ϕ parametrizes a family of patches that are isometric to the given development.

4.2. Cones

Let $\bar{\Gamma}$ be a planar conical patch (i.e. $\bar{c} = \text{const}$) where the ruling directions are parametrized by arc length, i.e., $|d'| = 1$. We determine a family of cones Γ isometric to $\bar{\Gamma}$ by elevating its vertex c while keeping its boundary b in the xy-plane.

Let us w.l.o.g. assume that the vertex is given by $c = (0, 0, h)$ and the ruling direction by

$$d(s) = (\cos\phi(s)\cos\theta(s), \cos\phi(s)\sin\theta(s), \sin\phi(s)).$$

The curve b lies in the xy-plane if

$$0 = b_z = h + l\sin\phi \quad\Longrightarrow\quad \phi = -\arcsin\frac{h}{l}.$$

As isometry preserves arc length, we conclude

$$1 = |\bar{d}'|^2 = |d'|^2 = \phi'^2 + \theta'^2\cos^2\phi,$$

and therefore

$$\theta' = \frac{\sqrt{1-\phi'^2}}{|\cos\phi|} = \frac{\sqrt{l'^2h^2 - (l^2-h^2)l'^2}}{l^2-h^2}.$$

The square root is real if $|h| < h_{\max}$, where

$$h_{\max} = \min_{s\in[s_0,s_1]} \frac{l^2}{\sqrt{l'^2+l^2}},$$

and thus feasible values for h parametrize a one-parameter family of cones that are isometric to a given development.

4.3. Tangent developables

Finally, let $\bar{\Gamma}$ be a planar patch of a tangent developable where the curve of regression is parametrized by arc length. We denote the curvature of $\bar{c}$ by κ. As before, we determine a tangent developable Γ isometric to $\bar{\Gamma}$ by keeping b planar and elevating the regression curve c.

Again, we require that the z-coordinate of b vanishes, i.e.,

$$0 = b_z = c_z + lc_z' \quad\Longrightarrow\quad c_z = he^{-\int_{s_0}^{s}\frac{1}{l}dt} =: hL, \tag{1}$$

where $h = c_z(s_0)$. As parametrization and curvature of c must be preserved, we conclude

$$|c'| = \sqrt{c_x'^2 + c_y'^2 + c_z'^2} = 1, \tag{2}$$

and

$$|c''| = \sqrt{c_x''^2 + c_y''^2 + c_z''^2} = |\kappa|. \tag{3}$$

We extract c_y' from Equation (2) and obtain by derivation

$$c_y'' = -\frac{c_x'c_x'' + c_z'c_z''}{\sqrt{1-c_x'^2-c_z'^2}} = -\frac{1}{c_y'}\left(c_x'c_x'' + c_z'c_z''\right). \tag{4}$$

Rewriting Equations (3) and (4) yields

$$c_x'' = \frac{1}{-1+c_z'^2}\left(c_x'c_z'c_z'' + c_y'\sqrt{\kappa^2(1-c_z'^2) - c_z''^2}\right),$$
$$c_y'' = \frac{1}{-1+c_z'^2}\left(c_y'c_z'c_z'' - c_x'\sqrt{\kappa^2(1-c_z'^2) - c_z''^2}\right),$$

i.e., a linear system of differential equations of first order for c_x'' and c_y'', namely,

$$c_x'' = \;\; a(s)c_x' + b(s)c_y',$$
$$c_y'' = -b(s)c_x' + a(s)c_y'.$$

The solutions for initial values $c_x'(s_0) = x_0$ and $c_y'(s_0) = y_0$, corresponding to the rotational position of the curve, read

$$c_x' = e^{A(s)}(x_0\cos B(s) + y_0\sin B(s)),$$
$$c_y' = e^{A(s)}(-x_0\sin B(s) + y_0\cos B(s)),$$

where

$$A(s) = \int_{s_0}^{s} a(\sigma)d\sigma \quad\text{and}\quad B(s) = \int_{s_0}^{s} b(\sigma)d\sigma.$$

The square root appearing in $B(s)$, or $b(s)$ resp., is real-valued, as long as

$$c_z''^2 < \kappa^2\left(1 - c_z'^2\right).$$

Inserting Equation (1) implies

$$\frac{L^2}{l^4}(1+l')^2h^2 < \kappa^2\left(1 - \frac{L^2}{l^2}h^2\right).$$

Finally, this yields an upper bound for $|h| \le h_{\max}$, namely,

$$h_{\max} = \min_{s\in[s_0,s_1]} \frac{\kappa L l^2}{\sqrt{\kappa^2 l^2 + (1+l')^2}},$$

as we then just need to integrate c_x' and c_y', whose initial values correspond to the location of the curve.

Interpretation. We can visualize the deforming process as a smooth, isometric elevation of the developable surface from its planar configuration. In case of a cylinder, we also give the maximal elevation angle for the ruling direction, in case of a cone the maximal height of the vertex and in case of a tangent developable the maximal height of the initial point of the striction curve. Exceeding those values would "break" the surfaces.

Remark. The method shown above can be adapted for other types of input data, e.g., c being not arc length parametrized or not a profile curve, vertex or curve of regression. For simplicity, we aimed to show our approach only for these adapted cases.

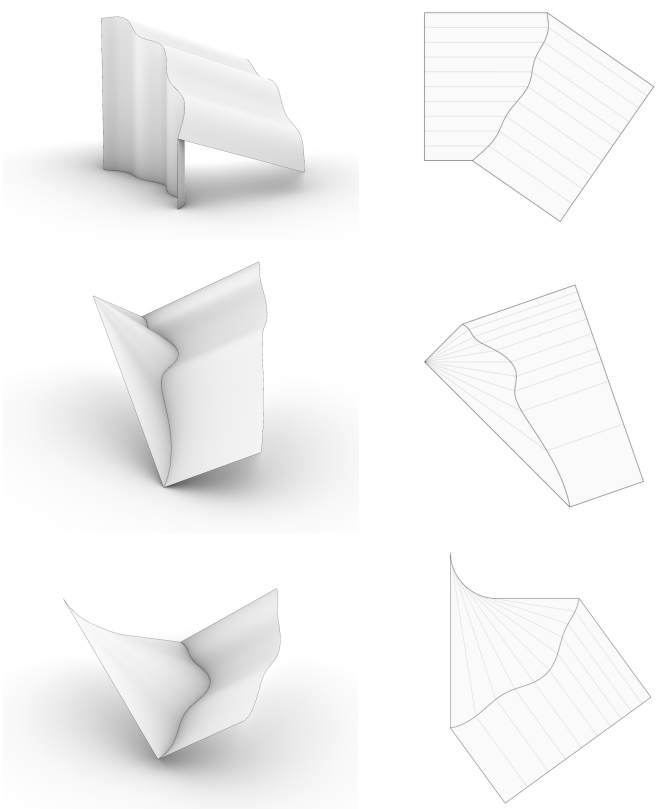

Figure 3: The basic types of developable surfaces folded into cylinders.

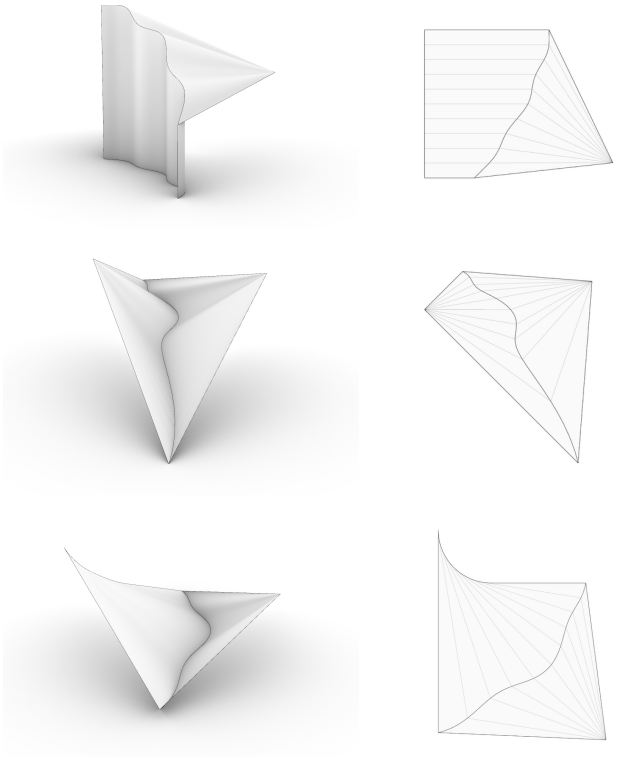

Figure 4: The basic types of developable surfaces folded into cones.

5. Creases into Cylinders and Cones

Comparing lengths, and not curvatures, our method determines the crease curves that fold a given developable surface into cylinders and cones with prescribed ruling directions and vertices in space and development.

In the following, we consider two developable surfaces Γ_A and Γ_B and indicate their quantities with a corresponding subscript.

We make the ansatz that the fold curve f on a first surface Γ_A is parametrized by

$$f(s) = c_A(s) + l_A(s)d_A(s),$$

where $l_A(s)$ is an unknown length function. Here, c_A can be any and not necessarily arc length parametrized curve on Γ_A and d_A the corresponding ruling directions. Again, let $\bar{c}_A$ and $\bar{d}_A$ denote their developments with $|\bar{c}'_A| = |c'_A|$ and $|\bar{d}_A| = |d_A|$. We assume the corresponding development to be given by

$$\bar{f}(s) = \bar{c}_A(s) + l_A(s)\bar{d}_A(s).$$

5.1. Folds into cylinders

Let the second surface be a cylinder Γ_B which is given by its ruling direction d_B and its developed directions $\bar{d}_B$. We make the assumption, that its profile curve $c_B(s)$ can be derived by another unknown function $l_B(s)$ from

$$c_B(s) = f(s) + l_B(s)d_B \quad \text{and} \quad \bar{c}_B = \bar{f}(s) + l_B(s)\bar{d}_B.$$

We fix the two planes containing c_B and $\bar{c}_B$ resp. by two scalars k and $\bar{k}$ and derive the unknown functions l_A and l_B from the resulting planarity constraints

$$k := c_B \cdot d_B \quad \text{and} \quad \bar{k} := \bar{c}_B \cdot \bar{d}_B.$$

Solving yields for $x = d_A \cdot d_B - \bar{d}_A \cdot \bar{d}_B \neq 0$,

$$l_A = \frac{1}{x}\left(k - \bar{k} - c_A \cdot d_B + \bar{c}_B \cdot \bar{d}_B\right), \tag{5}$$

$$l_B = \frac{1}{x}\left((k - c_A \cdot d_B)\,\bar{d}_A \cdot \bar{d}_B - \left(\bar{k} - \bar{c}_A \cdot \bar{d}_B\right) d_A \cdot d_B\right). \tag{6}$$

Examples are shown in Fig. 3.

5.2. Folds into cones

Let the second surface Γ_B be a cone with vertex c_B and its developed counterpart $\bar{c}_B$. Then the isometry condition

$$|f - c_B|^2 = |\bar{f} - \bar{c}_B|^2$$

yields the lengths

$$l_A = \frac{1}{2}\frac{|\bar{c}_A - \bar{c}_B|^2 - |c_A - c_B|^2}{(c_A - c_B) \cdot d_A - (\bar{c}_A - \bar{c}_B) \cdot \bar{d}_A}. \tag{7}$$

Examples are shown in Fig. 4.

Remarks. Our method avoids computing the Frenet frames of the crease curves as it just uses information about lengths. It can also be utilized to compute multiple consecutive folds into either cylinders or cones by prescribing their ruling direction or apexes.

However, the obtained surfaces may exhibit self-intersections. Furthermore, we may obtain infinite lengths l_A if the input data is chosen "unnaturally", e.g., if the second cones apex lies on one of the first cones rulings and the crease passes trough their midpoint.

Unfortunately, this method may not be applicable for folds into tangent developables as we would have to consider the second curve's parametrization.

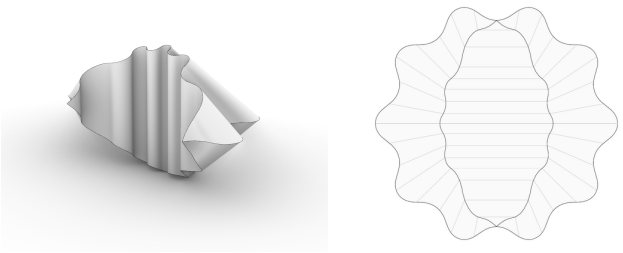

(a) Generalization of the folded Vesica Piscis shape.

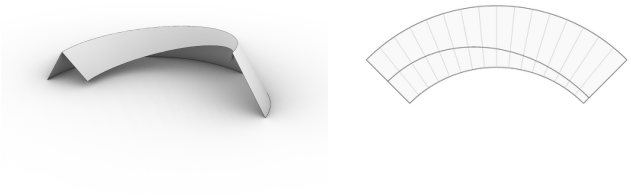

(b) Huffman's reflected cones.

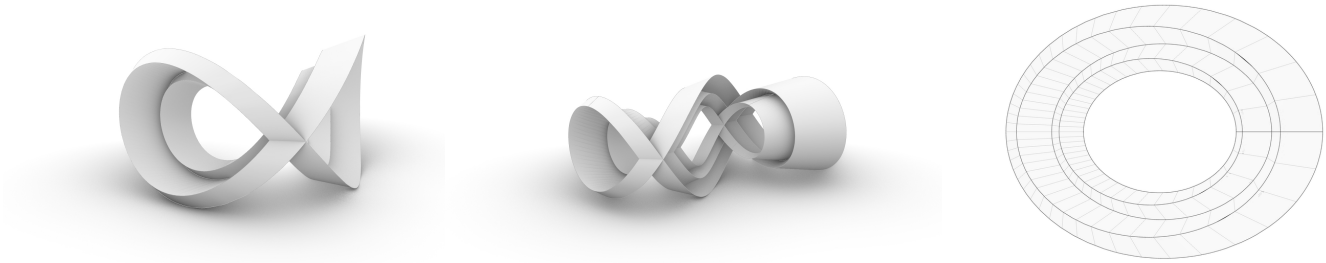

(c) Examples of closed states of Huffman's design of a fold between two cones of constant angle using elliptical crease curves.

Figure 5: Illustrations of examples in Section 6.

6. Applications and Examples

6.1. Vesica Piscis like shapes

The folded Vesica Piscis was obtained by parametrizing one half of the development as a cone with vertex in the center of the patch. Then, the cone was determined by elevating the vertex of the given surface patch, while keeping its boundary in the xy-plane. Finally, the obtained cone was folded into a cylinder with z-parallel rulings and reflected on the xy-plane. This procedure can be easily generalized to more complicated symmetric patches, see Fig. 5(a) for an example.

6.2. Parametrization of Huffman's reflected cones

We can use the computations above to determine the parametrization of the folds of cones of revolution into cones, whose developed vertices coincide. It is well known that this results in a planar crease curves with reflecting rule lines and a parametrization of the crease curve can be obtained by referring to standard literature on geometry about conical sections. Nevertheless, we would like to illustrate the simplicity of our tools on this example and hereby offer another point of view, see Fig. 5(b).

Let us start with a cone of revolution Γ_A with vertex $c_A = (0, 0, \sin\theta)$ where θ denotes the opening angle, i.e.,

$$d_A(s) = \left(\cos\theta\cos\frac{s}{\cos\theta}, \cos\theta\sin\frac{s}{\cos\theta}, \sin\theta\right).$$

Its development is given by

$$\bar{c}_A = (0, 0) \quad \text{and} \quad \bar{d}_A(s) = (\cos s, \sin s).$$

We compute the fold of Γ_A into Γ_B, whose developed vertex coincides with the origin, $\bar{c}_B = (0, 0)$. We ensure that the crease curve passes through $c_A + d_A(0)$ by parametrizing the location of c_B with

$$c_B = (\cos\theta, 0, 0) + (\cos\beta, 0, \sin\beta).$$

Inserting into Equation (7) yields the length function of the crease curve,

$$l_A = \frac{1 + \cos\beta\cos\theta + \sin\beta\sin\theta}{\cos\frac{s}{\cos\theta}\cos\theta(\cos\beta + \cos\theta) + \sin\theta(\sin\beta + \sin\theta)}.$$

Computing

$$f \cdot (c_B - c_A) = \cos\theta(\cos\beta + \cos\theta),$$

shows that the crease curve lies in the bisecting plane of c_A and c_B and thus the second cone Γ_B is also a cone of revolution since the rulings are reflected. This method can be used for successive creases as well.

6.3. Huffman's folded ellipses

It is shown in [10] that scaled ellipses sharing a common focal point fold with reflecting rulings that converge to the corresponding focal points. The reflecting ruling property yields a fold of constant angle between two cones. Those curves are characterized those curves as geodesics on rotational ellipsoids whose focal points correspond to the apexes of the cones, see [11].

We work on obtaining explicit parametrizations of geodesics on rotational ellipsoids from our formulas to show that there are fold angles, at which the obtained shape closes (disregarding self intersections), see Fig. 5(c).

6.4. Columns and tessellations

The above developed formulas can be used for the design of different types of curved crease origami shapes. For example, by consecutively folding surfaces into cylinders at suitable angles, column-like shapes can be obtained. Design inspirations can be found in [23]. However, we are not restricted to the rulings being perpendicular to the axis of rotation. Moreover, one can design segments and arrange them to tessellations. We give two examples in which we tessellate a cylinder and a plane.

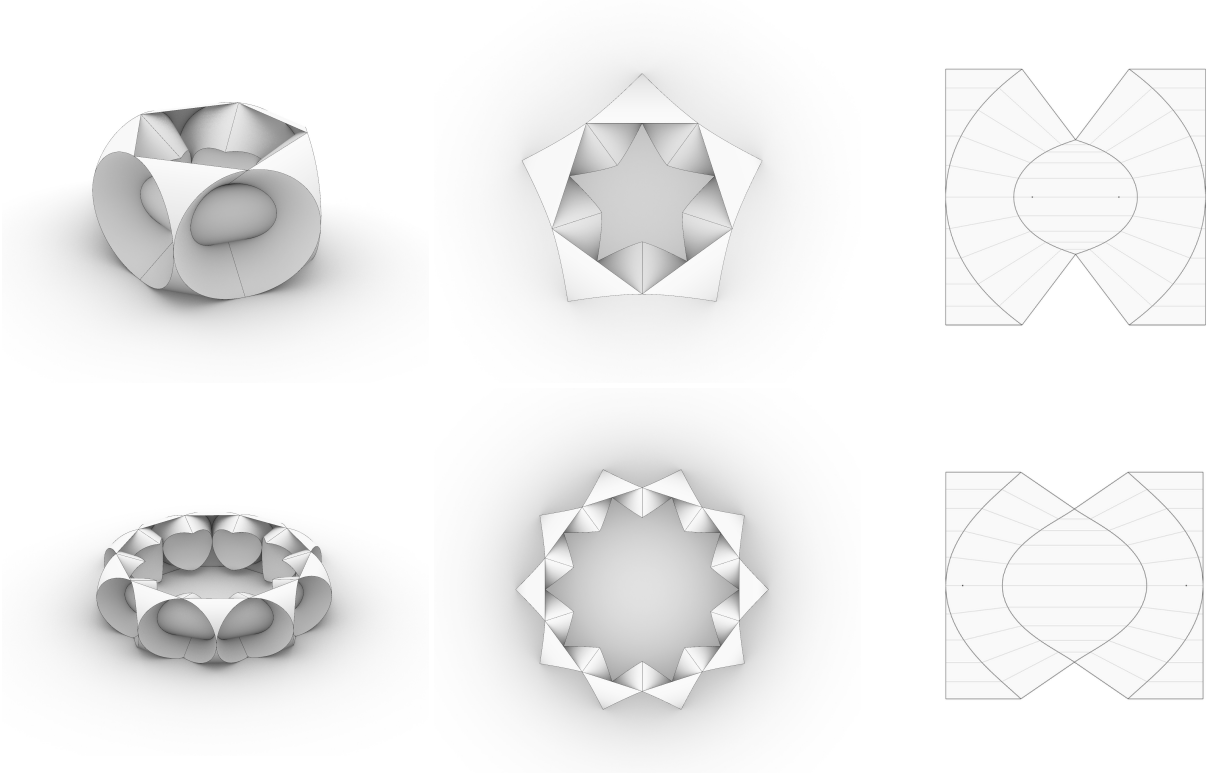

Figure 6: Folded stars with $n = 5$ and $n = 10$.

6.4.1. Star Columns

We illustrate the convenience of mathematical curved crease origami design by the following example. We fold a right circular cone into two cylinders at suitable angles such that the resulting shape has a star shaped opening in its center, see Fig. 6.

We start by arranging $n > 3$ cones of revolution around the origin, i.e., $c_A = (0, 0, 0)$. One representative's ruling directions are given by

$$d_A = \left(\sin\theta, \cos\theta\cos\frac{s}{\cos\theta}, \cos\theta\sin\frac{s}{\cos\theta}\right),$$

where $\theta = \frac{\pi}{2} - \frac{\pi}{n}$ and $s \in [-\frac{\pi}{2}\cos\theta, \frac{\pi}{2}\cos\theta]$. Furthermore, we fix its development

$$\bar{c}_A = (0, 0) \quad \text{and} \quad \bar{d}_A = (\cos s, \sin s)\,.$$

Firstly, we fold this cone into a cylinder with

$$d_{B_1} = (0, -1, 0) \quad \text{and} \quad \bar{d}_{B_1} = (-1, 0).$$

We set the initial point of the crease curve $f_1(0)$ at $d_A(0)$ by setting the profile curve to be in the plane $y = 0$, thus

$$k_1 = 0,$$
$$\bar{k}_1 = \left(\bar{d}_A(0) + \cos\theta\,\bar{d}_{B_1}\right)\cdot\bar{d}_{B_1} = -1 + \cos\theta.$$

The lengths in Equation (5) therefore simplify to

$$l_{A_1} = \frac{-1 + \sin\frac{\pi}{n}}{-\cos s + \cos\frac{s}{\sin\frac{\pi}{n}}\sin\frac{\pi}{n}} \quad \text{and} \quad l_{B_1} = \cos\frac{s}{\sin\frac{\pi}{n}}\sin\frac{\pi}{n} l_{A_1}.$$

Secondly, we fold the cone into a cylinder with

$$d_{B_2} = \left(\sin\frac{\pi}{n}, \cos\frac{\pi}{n}, 0\right) \quad \text{and} \quad \bar{d}_{B_2} = (1, 0).$$

As we would like the xy-projected outer rulings of the second cylinder to pass trough the tip of the star, we introduce a new parameter k_x as the starting point of the crease, i.e.,

$$k_2 = k_x d_A(0)\cdot d_{B_2} = k_x\cos\frac{n\theta + \pi}{n},$$
$$\bar{k}_2 = k_x\bar{d}_A(0)\cdot\bar{d}_{B_2} = k_x.$$

The lengths then simplify to

$$l_{A_2} = \frac{k_x}{\cos s + \cos\frac{\pi}{n}\sin\frac{\pi}{n}(1 - \cos\frac{s}{\sin\frac{\pi}{n}})},$$
$$l_{B_2} = \cos\frac{\pi}{n}\sin\frac{\pi}{n}\left(1 - \cos\frac{s}{\sin\frac{\pi}{n}}\right) l_{A_2}.$$

The outer rulings of the cylinder are aligned with the tips if the x or y coordinates of $f_2(s_0) + l_{B_2}(s_0)d_{B_2}$ and $c_{B_1}(0)$ are the same. Solving for k_x yields

$$k_x = \frac{\cos\left(\frac{\pi}{2}\sin\frac{\pi}{n}\right)}{\cos^2\frac{\pi}{n}} + \tan\frac{\pi}{n} > 1 \quad \text{for} \quad n = 3, 4, \ldots$$

6.4.2. Tessellating a cylinder of revolution

The aim of this example is to tessellate two cylinders of revolution with curved creases. We fold the outer cylinder, which is w.l.o.g. of radius 1, into a cone with its vertex lying on the axis of the cylinder. Then the second crease curve is obtained by scaling the first crease onto the inner cylinder. It is convenient to restrict the parameter to $s \in [-\frac{\pi}{n}, \frac{\pi}{n}]$ for $n > 3$. Then, by reflection w.r.t. a xy-parallel plane, we obtain one inner lens-shaped segment of the tessellation, which can then be used to row-wise cover the

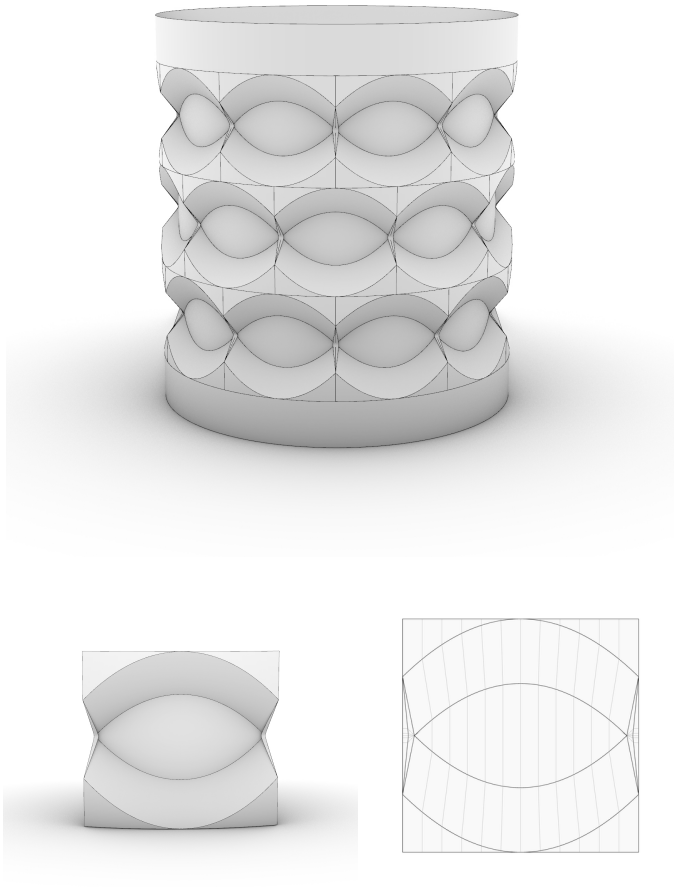

Figure 7: Example of a tessellation between two cylinders of revolution.

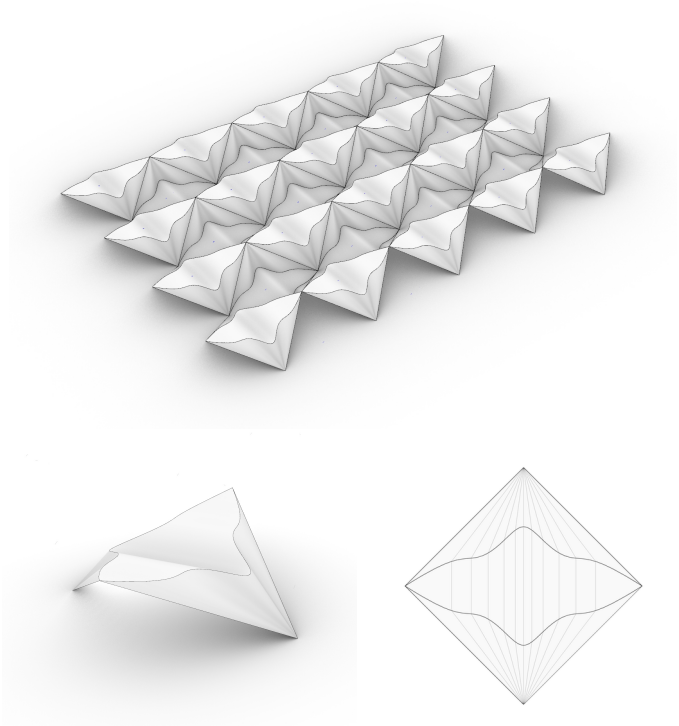

Figure 8: Example of a generalization of Huffman's tessellation of the plane.

cylinders. However, this design leaves a rhombic piece of paper between the lens vertices unused. There are many options how to treat those parts. We decided to fill the remaining space with a vertical lens obtained by folding a hyperbolic cylinder into a cone. However, as the rhombi become very narrow it would be also convenient to cut them out.

6.4.3. Generalizing Huffman's lens tessellation

We can also use the above discussed methods for "generalized" lens tessellations. Our approach differs from the computations in [9], where a crease ruling pattern without inflection points is folded into a kite. We, on the other hand, firstly establish the shape of one cone with developed opening angle $\frac{\pi}{2}$ that is then folded into a cylinder and, by reflection, folded back into a cone. Although our approach can also design crease curves with inflection points, we cannot guarantee the absence of self intersections. By reflecting and translating this segment, a planar tessellation can be obtained.

The example in Fig. 8 was obtained by sliding a cone with ruling lengths $l(s) = 2 + 0.15\cos(8s)$ to $h = 0.6h_{\max}$ and folding it into a cylinder with rulings of an angle of inclination of $\phi = -0.43\pi$ and suitable cutting.

7. Discussion

We have proposed two new concepts. Firstly, we investigated smoothly deformed developable surfaces in a mathematically rigorous way by sliding surface patches isometrically while keeping one boundary curve planar. The benefit is the explicit smooth description of the obtained surfaces and their developments. Our method differs from other interactive methods as they either discretize the surfaces or optimize for developability and isometry to a given patch and are thus just approximations. Secondly, we give simple formulas for the parametrization of crease curves of all types of developable surfaces into cylinders and cones. It is therefore possible to compute the crease curve by specifying a ruling direction or vertex in space and development. The advantage of this type of computational approach is among others the trivial control of the striction curve of the developable surface, which is one of the issues encountered in optimization based methods. As far as we know, this might be the first mathematically explicit technique to interactively treat multiple crease curves.

7.1. Limitations

Although our method is explicit and thus not burdened with computational issues, we unfortunately cannot prevent self-intersecting surfaces and crease curves escaping to infinity. However, we can use these computations to gain more insights into the behaviour of creased paper and for reasonably chosen input this method gives exact smooth representations of surfaces.

7.2. Future Work

We are interested in a better understanding of the behaviour of curved folds of developable surfaces, in particular the existence of curved crease Origami shapes. The next logical step is the investigation of folds into tangent surfaces within this framework. Furthermore, we would also like to explore possible applications to other disciplines, where exact developability and curved creases are necessary.

8. Acknowledgements

I gratefully acknowledge the support of the SFB-Transregio programme Geometry and Discretization (Austrian Science Fund grant no. I 2978). Furthermore, I would like thank Helmut Pottmann and Christian Müller for fruitful discussions and helpful remarks and Tony Wills for initiating this research about Susan Latham's inspiring sculpture. Moreover, I would like to thank Yves Klett and Jason Ku for their motivation and comments on the tessellation between two cylinders.

References

[1] K. Mundilova, T. Wills, Folding the vesica piscis, in: Proceedings of Bridges 2018: Mathematics, Art, Music, Architecture, Education, Culture, 2018, pp. 535–538.

[2] E. Demaine, M. Demaine, V. Hart, G. Price, T. Tachi, (Non)existence of pleated folds: How paper folds between creases, Graphs and Combinatorics 27 (3) (2011) 377–397.

[3] M. Dias, L. Dudte, L. Mahadevan, C. Santangelo, Geometric mechanics of curved fold origami, Physical Review Letters 109 (2012).

[4] M. Dias, C. Santangelo, The shape and mechanics of curved-fold origami structures, Europhysics Letters 100 (2012).

[5] E. Demaine, M. Demaine, D. Koschitz, Reconstructing David Huffman's legacy in curved-crease folding, The Americal Mathematical Monthly 106 (1999) 27–35.

[6] D. Koschitz, Computational design with curved creases: David Huffman's approach to paperfolding, Ph.D. thesis, Massachusetts Institute of Technology (2014).

[7] D. Huffman, Curvature and creases: A primer on paper, IEEE Transactions on Computers C-25 (1976) 1010–1019.

[8] D. Fuchs, S. Tabachnikov, More on paperfolding, The Americal Mathematical Monthly 106 (1999) 27–35.

[9] E. Demaine, M. Demaine, D. Huffman, D. Koschitz, T. Tachi, Characterization of curved creases and rulings: Design and analysis of lens tessellations, in: Origami6: Proceedings of the 6th International Meeting on Origami in Science, Mathematics and Education (OSME), Vol. 1, 2014, p. 209–230.

[10] E. Demaine, M. Demaine, D. Huffman, D. Koschitz, T. Tachi, Conic crease patterns with reflecting rule lines, in: Origami^7: Proceedings of the 7th International Meeting on Origami in Science, Mathematics and Education (OSME 2018), Vol. 2, Oxford, England, 2018, pp. 573–590.

[11] W. Wunderlich, Raumkurven, die pseudogeodätische Linien zweier Kegel sind, Monatsh. Math. 54 (1950) 55–70.

[12] W. Wunderlich, Raumkurven, die pseudogeodätische Linien eines Zylinders und eines Kegels sind, Compos. Math. 8 (1950).

[13] W. Wunderlich, Pseudogeodätische Linien auf Kegelflächen, Sitzungsber., Abt. II, österr. Akad. Wiss., Math.-Naturw. Kl. 158 (1950) 75–105.

[14] W. Wunderlich, Pseudogeodätische Linien auf Zylinderflächen, Sitzungsber., Abt. II, österr. Akad. Wiss., Math.-Naturw. Kl. 158 (1950) 61–73.

[15] O. Röschel, Curved folding with pairs of cylinders, Journal for Geometry and Graphics 21 (2017) 193–200.

[16] O. Röschel, Curved folding with pairs of cones, in: Proceedings of the 18th International Conference on Geometry and Graphics (ICGG), 2019, p. 381–388.

[17] J. Boersma, J. Molenaar, Geometry of the shoulder of a packaging machine, SIAM Review 37 (3) (1995) 406–422.

[18] J. Solomon, E. Vouga, M. Wardetzky, E. Grinspun, Flexible developable surfaces, in: Computer Graphics Forum, Vol. 31, Oxford, UK, 2012, pp. 1567–1576.

[19] A. Ghassaei, E. Demaine, N. Gershenfeld, Fast, interactive origami simulation using GPU computation, in: Origami^7: Proceedings of the 7th International Meeting on Origami in Science, Mathematics and Education (OSME 2018), Vol. 4, Oxford, England, 2018, pp. 1151–1167.

[20] T. Tachi, G. Epps, Designing one-DOF mechanisms for architecture by rationalizing curved folding, in: Proceedings of the International Symposium on Algorithmic Design for Architecture and Urban Design, (ALGODE), 2011.

[21] T. Tachi, Composite rigid-foldable curved origami structure, in: Proceedings of Transformables, 2013.

[22] J. Mitani, T. Igarashi, Interactive design of planar curved folding by reflection, in: Pacific Graphics, 2011.

[23] J. Mitani, Column-shaped origami design based on mirror reflectons, Journal for Geometry and Graphics 16 (2012) 185–194.

[24] M. Kilian, S. Flöry, Z. Chen, N. J. Mitra, A. Sheffer, H. Pottmann, Curved folding, ACM Transactions on Graphics 27 (3) (2008) #75, 1–9.

[25] C. Tang, P. Bo, J. Wallner, H. Pottmann, Interactive design of developable surfaces, ACM Trans. Graph. 35 (2) (2016) 12:1–12:12.

[26] M. Rabinovich, T. Hoffmann, O. Sorkine-Hornung, Discrete geodesic nets for modeling developable surfaces, ACM Trans. Graph. 37 (2) (2018) 16:1–16:17.

[27] M. Kilian, A. Monszpart, N. Mitra, String actuated curved folded surfaces, ACM Trans. Graph. 36 (4) (May 2017).

[28] T. Wills, D-forms: 3d forms from two 2d sheets, in: Bridges London: Mathematics, Music, Art, Architecture, Culture, London, 2006, pp. 503–510.

[29] H. Pottmann, J. Wallner, Computational Line Geometry, Springer-Verlag, Berlin Heidelberg, 2001.

[30] E. Demaine, G. Price, Generalized D-forms have no spurious creases, Discrete & Computational Geometry 43 (1) (2009) 179–186.

[31] H. Stachel, Two examples of solids constructed from given developments, Journal for Geometry and Graphics 20 (2016) 225–241.